Published in final edited form as:
Leukemia. 2014 March ; 28(3): 680–689. doi:10.1038/leu.2013.231.

Histone deacetylase 3 (HDAC3) as a novel therapeutic target in multiple myeloma

Jiro Minami[1,4], **Rikio Suzuki**[1,4], **Ralph Mazitschek**[2], **Gullu Gorgun**[1], **Balaram Ghosh**[2,3], **Diana Cirstea**[1], **Yiguo Hu**[1], **Naoya Mimura**[1], **Hiroto Ohguchi**[1], **Francesca Cottini**[1], **Jana Jakubikova**[1], **Nikhil C. Munshi**[1], **Stephen J. Haggarty**[3], **Paul G. Richardson**[1], **Teru Hideshima**[1], and **Kenneth C. Anderson**[1]

[1]Jerome Lipper Multiple Myeloma Center, Department of Medical Oncology, Dana-Farber Cancer Institute, Harvard Medical School, 450 Brookline Avenue, Boston MA 02215

[2]Center for Systems Biology, Massachusetts General Hospital, 185 Cambridge Street Suite 5.210, Boston, MA 02114

[3]Center for Human Genetic Research, Massachusetts General Hospital, Harvard Medical School, 185 Cambridge Street, Boston, Massachusetts 02114

Abstract

Histone deacetylases (HDACs) represent novel molecular targets for the treatment of various types of cancers, including multiple myeloma (MM). Many HDAC inhibitors have already shown remarkable anti-tumor activities in the preclinical setting; however, their clinical utility is limited due to unfavorable toxicities associated with their broad range HDAC inhibitory effects. Isoform-selective HDAC inhibition may allow for MM cytotoxicity without attendant side effects. In this study, we demonstrated that HDAC3 knockdown and a small molecule HDAC3 inhibitor BG45 trigger significant MM cell growth inhibition via apoptosis, evidenced by caspase and PARP cleavage. Importantly, HDAC3 inhibition downregulates phosphorylation (tyrosine 705 and serine 727) of STAT3. Neither IL-6 nor bone marrow stromal cells overcome this inhibitory effect of HDAC3 inhibition on p-STAT3 and MM cell growth. Moreover, HDAC3 inhibition also triggers hyperacetylation of STAT3, suggesting crosstalk signaling between phosphorylation and acetylation of STAT3. Importantly, inhibition of HDAC3, but not HDAC1 or HDAC2, significantly enhances bortezomib-induced cytotoxicity. Finally, we confirm that BG45 alone and in combination with bortezomib trigger significant tumor growth inhibition in vivo in a murine xenograft model of human MM. Our results indicate that HDAC3 represents a promising therapeutic target, and validate a prototype novel HDAC3 inhibitor BG45 in MM.

Corresponding Authors: Kenneth C. Anderson, MD, 450 Brookline Avenue, Mayer 557, Boston MA, 02215, Phone: 617-632-2144, Fax: 617-632-2140, kenneth_anderson@dfci.harvard.edu.
[4]Equally contributed to this manuscript

Conflict-of-interest disclosure: R.M. has financial interests in SHAPE Pharmaceuticals and Acetylon Pharmaceuticals. He is also the inventor on IP licensed to these two entities. P.G.R. is a member of advisory board for Celgene, Millennium, Johnson & Johnson, Novartis and Keryx. T.H. is a consultant for Acetylon Pharmaceuticals. K.C.A. is a member of advisory committees for Onyx, Celgene, Gilead, and Sanofi-Aventis, and is a scientific founder of Acetylon and Oncopep. Other authors declare no competing financial interests.

Keywords

multiple myeloma; histone deacetylase 3; STAT3; bortezomib

Introduction

A major challenge for molecular targeted therapy in multiple myeloma (MM) is its genetic complexity and molecular heterogeneity. Gene transcription within the tumor cell and its microenvironment can also be altered by epigenetic modulation (i.e., acetylation and methylation) in histones, and inhibition of histone deacetylases (HDACs) has therefore emerged as a novel targeted treatment strategy in MM and other cancers [1]. Histone deacetylases are divided into 4 classes: class-I (HDAC1, 2, 3, 8), class-IIa (HDAC4, 5, 7, 9), class-IIb (HDAC6,10), class-III (SIRT1–7), and class-IV (HDAC11). These classes differ in their subcellular localization (class-I HDACs are nuclear and class-II enzymes cytoplasmic), and their intracellular targets. Moreover, recent studies have identified non-histone targets of HDACs in cancer cells associated with various functions including gene expression, DNA replication and repair, cell cycle progression, cytoskeletal reorganization, and protein chaperone activity.

Several HDAC inhibitors (HDACi) are currently in clinical development in MM [2], and both vorinostat (SAHA) and romidepsin (FK228 or FR901228) have already received approval by the Food and Drug Administration (FDA) for the treatment of cutaneous T-cell lymphoma [3]. Vorinostat is a hydroxamic acid based HDACi that, like other inhibitors of this class including panobinostat (LBH589) and belinostat (PXD101), are generally non-selective with activity against class-I, II, and IV HDACs[4]. The natural product romidepsin is a cyclic tetrapeptide with HDAC inhibitory activity primarily towards class-I HDACs. Other HDACi based on amino-benzamide biasing elements, such as mocetinostat (MGCD103) and entinostat (MS275), are highly specific for HDAC1, 2 and 3. Importantly, clinical trials with non-selective HDACi such as vorinostat combined with bortezomib have shown efficacy in MM, but have attendant fatigue, diarrhea, and thrombocytopenia [5].

Our preclinical studies characterizing the biologic impact of isoform selective HDAC6 inhibition in MM, using HDAC6 knockdown and HDAC6 selective inhibitor tubacin [6], showed that combined HDAC6 and proteasome inhibition triggered dual blockade of aggresomal and proteasomal degradation of protein, massive accumulation of ubiquitinated protein, and synergistic MM cell death. Based upon these studies, a potent and selective HDAC6 inhibitor ACY-1215 [7] was developed, which is now demonstrating promise and tolerability in phase I/II clinical trials in MM [8]. In this study, we similarly determine whether isoform inhibition of class-I HDAC mediates cytotoxicity, without attendant toxicity to normal cells. We define the role of HDAC3-selective inhibition in MM cell growth and survival using both lentiviral HDAC3 knockdown and a novel small molecule HDAC3-selective inhibitor BG45. Within class-I HDACs, our results show that HDAC3 represents a promising therapeutic target in MM, and that combined HDAC3 and proteasome inhibition mediates synergistic cytotoxicity. Our studies provide the preclinical

rationale for derived clinical trials using HDAC3 selective inhibitors to both enhance MM cytotoxicity and improve tolerability.

Methods

Reagents

Non-selective HDAC inhibitors LBH589 (panobinostat) and MS275 (entinostat), as well as HDAC6 selective inhibitor tubastatin-A were purchased from Selleck Chemicals (Houston, TX). Bortezomib was also obtained from Selleck Chemicals. BG45 (*N*-(2-aminophenyl)pyrazine-2-carboxamide) and Merck60 (4-acetamido-*N*-(2-amino-5-(thiophen-2-yl)phenyl)benzamide) (PMID: 18182289) were synthesized in house (Massachusetts General Hospital, Cambridge, MA). Human recombinant Interleukin (IL)-6 was purchased from R & D Systems (Minneapolis, MN).

Cells

RPMI8226 and U266 human MM cell lines, as well as human embryonic kidney 293T cells, were obtained from American Type Culture Collection (ATCC). MM.1S cells were kindly provided by Dr. Steven Rosen (Northwestern University). Interleukin-6 dependent INA-6 cell line was obtained from Dr. Renate Burger (Univ. of Kiel, Kiel, Germany). Melphalan-resistant (LR5) and doxorubicin-resistant (RPMI-DOX40) cells were kindly provided by Dr. William Dalton (Lee Moffitt Cancer Center). OPM1 and OPM2 cells were obtained from Dr. Edward Thompson (University of Texas Medical Branch, Galveston, TX). MM cell lines were maintained in RPMI 1640 medium (Sigma-Aldrich) supplemented with 10% fetal bovine serum, 2mM L-glutamine (Invitrogen), 100 units/mL penicillin, and 100 units/mL streptomycin (Invitrogen). 293T cells were maintained in Dulbecco Modified Eagle Medium (Sigma-Aldrich) supplemented with 10% fetal bovine serum, 100 units/mL penicillin, and 100 mg/mL streptomycin (Invitrogen).

BM specimens were obtained from patients with MM, and mononuclear cells (MNCs) were separated by Ficoll-Hipaque density sedimentation. Primary CD138+ plasma cells from MM patients were obtained using negative selection, as in previous studies [9] CD138- BMMNCs were used to establish long-term BMSC cultures, as previously described [9]. Peripheral blood mononuclear cells were collected from healthy volunteers to obtain mononuclear cells (PBMCs). All procedures were performed with IRB-approved (Dana-Farber Cancer Institute) protocols and informed consent, and in accordance with the Declaration of Helsinki protocol.

Cell growth inhibition assay

The growth inhibitory effects of Merck60, MS275, BG-45, bortezomib and HDAC3 knockdown in MM cell lines were assessed by measuring 3-(4,5-dimethylthiazol-2-yl)-2,5-diphenyl tetrasodium bromide (MTT; Sigma-Aldrich) dye absorbance, as previously described [10]. To measure proliferation of MM cells, the rate of DNA synthesis was measured by ^{3}[H]-thymidine (Perkin-Elmer) uptake, as previously reported [10].

Immunoblotting and immunoprecipitation

MM cells were harvested and lysed using sodium dodecyl sulfate-polyacrylamide gel electrophoresis (SDS-PAGE) sample buffer containing 60 mM Tris-HCl, pH 6.8, 2% SDS, 10% glycerol, 0.005% bromophenol blue, 5 mM ethylenediaminetetraacetic acid, 5 mM NaF, 2 mM Na_3VO_4, 1 mM phenylmethylsulfonyl fluoride (PMSF), 5 μg/mL leupeptin, and 5 μg/mL aprotinin; and then heated at 100 °C for 5 min. After the determination of protein concentration using DC protein assay (Bio-Rad, Hercules, CA), β-mercaptoethanol (β-ME) was added to the whole-cell lysates to a 2% final β-ME concentration. The whole-cell lysates were subjected to SDS-PAGE, transferred to nitrocellulose membranes (Bio-Rad, Hercules, CA) or polyvinylidene fluoride membranes (Millipore, Billerica, MA), and immunoblotted with anti-histone H3, -HDAC1, -HDAC2, -HDAC3, -Acetyl-histone H2A (Lysine 5) (Ac-H2AK5), -Acetyl-histone H2B (lysine 5) (Ac-H2BK5), -Acetyl-histone H3 (lysine 9) (Ac-H3K9), -Acetyl-histone H4 (lysine 8) (Ac-H4K8), -glyceraldehyde-3-phosphate dehydrogenase (GAPDH), -poly (ADP-ribose) polymerase (PARP), -caspase-3, -caspase-8, -caspase-9, -Signal transducers and activators of transcription 3 (STAT3), -phospho-STAT3 (pSTAT3) (tyrosine 705), -pSTAT3 (serine 727), -p21, -Janus kinase 2 (JAK2), -acetylated-Lysine (Ac-K), and anti-phosphorylated-tyrosine antibodies (Abs; Cell Signaling Technology, Beverly, MA).

For immunoprecipitation, MM cells were lysed with Nonidet P-40 (NP-40) buffer (50 mM Tris-HCl [pH 7.4], 150 mM NaCl, 1% NP-40, 5 mM ethylenediaminetetraacetic acid, 5 mM NaF, 2 mM Na_3VO_4, 1 mM PMSF, 5 μg/mL leupeptin, and 5 μg/mL aprotinin). Whole-cell lysates were incubated with anti-STAT3, -JAK2, and -green fluorescent protein (GFP) Abs for 2 hours at 4°C, and then incubated with Protein A/G PLUS-Agarose® (Santa Cruz Biotechnology) overnight at 4°C. Anti-GFP Ab served as a control. Immune complexes were analyzed by immunoblotting with anti-STAT3, -JAK2, -acetylated-Lysine, and -phosphorylated-tyrosine Abs.

Transfection of short hairpin RNA (shRNA)

HDAC1, HDAC2 and HDAC3 pLKO.1 shRNA vectors were obtained from the RNA Interference Screening Facility at the Dana-Farber Cancer Institute. Recombinant lentivirus was produced and infection of MM cells was performed as previously described [11].

Synthesis of a small molecule HDAC3 inhibitor BG45

The procedure to generate BG45 is demonstrated in Supplemental Figure S2A.

Synthesis of *tert*-butyl (2-aminophenyl)carbamate (2)—To a stirring solution of benzene-1,2-diamine (1.0 g, 9.247 mmol) and 4-dimethylminopyridine (DMAP, 50mg) in THF (20 mL), a solution of di-tert-butyl dicarbonate (Boc_2O; 1.009g, 4.6236 mmol) in dichloromethane (20mL) was added drop wise at room temperature. The reaction mixture was evaporated in a rotary evaporator and purified by column chromatography using hexane and ethylacetate solvent mixture (80:20) to obtain the desired mono-Boc protected compound 2 (0.380 g, 20% yield).

Synthesis of *tert*-butyl (2-(pyrazine-2-carboxamido)phenyl)carbamate (3)— Compound 3 was synthesized following aromatic acid and aromatic amine coupling reactions, where pyrazine-2-carboxylic acid (0.03g, 0.242mmol) was dissolved in dichloromethane/pyridine (1:1) mixture, and EDCI (0.051g, 0.266 mmol) was added and stirred for 10 min. Tert-butyl (2-aminophenyl)carbamate (0.061g, 0.29 mmol) and catalytic amounts of 4-DMAP were added at room temperature, and stirring was continued to 2h. The reaction mixture was evaporated, and crude mixture was resuspended into ethyl acetate and extracted from aqueous $NaHCO_3$ solution. After evaporating the EtOAc layer, the titled compounds were purified by column chromatography using ethyl acetate methanol (9:1) solvent system to obtain the desired compound 3 (0.024 g, 31.6% yield).

Synthesis of *N*-(2-aminophenyl)pyrazine-2-carboxamide (4)—The final compound is made by deprotection of Boc group from *tert*-butyl (2-(pyrazine-2-carboxamido)phenyl)carbamate using dichloromethane and trifluoroacetic acid (1:1) mixture at room temperature for 30 min, which was then made free base by suspending the crude mixture into aq$NaHCO_3$ solution and extraction into dichloromethane. The organic layer was evaporated to obtain the pure final compound with quantitative yield (0.016 g). Inhibitory activity of BG45 against individual HDAC isoforms was determined as previously described [12].

Murine xenograft models

CB17 SCID mice (48–54 days old) were purchased from Charles River Laboratories (Wilmington, MA). All animal studies were conducted according to protocols approved by the Animal Ethics Committee of the Dana-Farber Cancer Institute. After irradiation (200cGy), mice were subcutaneously injected with 5×10^6 MM.1S cells in the right flank. BG45 and bortezomib were dissolved in 10% Dimethylacetamide (DMSA; Sigma-Aldrich) in 10% Kolliphor® HS15 (Sigma-Aldrich) in phosphate buffered saline (PBS) and 0.9% saline solution, respectively. When tumors were measurable, mice were treated with intraperitoneal injection (IP) of vehicle control, BG45 (15 mg/kg), or BG45 (50mg/kg) 5 days a week for 3 weeks (n=6/group). Additionally, mice were also treated with 50 mg/kg BG45 in combination with 0.5 mg/kg (subcutaneous injection) bortezomib twice a week. Tumor size was measured every three days, and tumor volume was calculated with the formula: $V=0.5(a\times b^2)$, where “a” is the long diameter of the tumor and “b” is the short diameter of the tumor. Mice were sacrificed when the tumor reached 2cm in length or $2cm^3$ volume, or if mice appeared moribund to prevent unnecessary morbidity. Survival was evaluated from the first day of the treatment until death.

Statistical analysis

The combined effect of drugs was analyzed by isobologram analysis using the Compusyn software program (ComboSyn, Inc.); a combination index (CI) < 1 is indicative of a synergistic effect. In the murine xenograft studies, statistical significance was determined by Student t test. The minimal level of significance was $p< 0.05$.

Results

MS275 is more cytotoxic than Merck60 in MM cells

Non-selective HDACi have demonstrated variable anti-MM activity in preclinical studies. We first examined the growth inhibitory effect of Merck60 (HDAC1, 2 inhibitor previously reported as compound #60 by Method *et al.* PMID 18182289) versus MS275 (HDAC1, 2, 3 inhibitor) in MM cell lines using MTT assay. MS275 triggered significant MM cell growth inhibition, whereas Merck60 induced only a modest growth inhibition effect (Figure 1A). Immunoblotting confirmed that all MM cell lines express HDAC1, 2, and 3 proteins (Figure 1B). We next examined the effects of these agents on acetylation of histones in RPMI8226 MM cells. Importantly, MS275 in a dose-dependent manner more potently induced acetylation of histones (H2A, H2B, H3 and H4) and increased $p21^{WAF1}$ expression than Merck60 (Figure 1C). These results suggest that HDAC3 plays an important role in MM cell growth and/or survival.

HDAC3 knockdown inhibits MM cell growth

To determine that the MM cell growth inhibitory effect of MS275 is predominantly due to HDAC3 inhibition, we next performed knockdown of HDAC isoforms (HDAC 1, 2, and 3) using a lentiviral shRNA infection system. We first confirmed isoform-selective HDAC1, 2, or 3 knockdown in RPMI8226 MM cells by immunoblotting (Figure 2A). Importantly, HDAC3 knockdown triggered the most significant growth inhibitory effect in RPMI8226 cells, assessed by both [^{3}H]-thymidine uptake (Figure 2B) and MTT assay (Figure 2C). In contrast, HDAC1 knockdown induced only modest growth inhibition, and no growth inhibitory effect was observed after HDAC2 knockdown, further confirming that HDAC3 plays a crucial role in MM cell growth and survival. The molecular mechanism whereby HDAC3 knockdown triggers MM cell growth inhibition was further examined. HDAC3, but not HDAC1 or 2, knockdown induces caspase-3 and PARP cleavage (Figure 2D). We also examined the effects of HDAC1, HDAC2 or HDAC3 knockdown on acetylation of histones in RPMI8226 cells. As shown in Figure 2E, there is no significant difference in the pattern of histone lysine acetylation between isoform-selective HDAC 1, 2 or 3 knockdown cells. Taken together, these results suggest that HDAC3 knockdown induces growth arrest and apoptosis. Similar results were also observed in MM.1S cells (Supplemental Figure 1).

HDAC3 modulates JAK/STAT3 pathway in MM cells

Previous studies have shown that HDAC3 alters STAT3 phosphorylation in other cell types [13, 14], and we have previously shown that JAK2/STAT3 pathway plays an important role in MM cell survival [15–18]. We therefore next first examined whether non-selective HDAC inhibitor LBH589 modulated p-STAT3 in MM cells. We observed that p-STAT3 was significantly inhibited by LBH589 treatment in MM.1S, U266, and INA-6 cells (Figure 3A). Since p-STAT3 can be upregulated in the context of the BM microenvironment, we examined whether inhibition of p-STAT3 by LBH589 treatment of MM.1S cells was maintained even in the presence of exogenous IL-6 or BMSC culture supernatants. Both IL-6 and BMSC culture supernatants markedly upregulated p-STAT3, which was blocked by LBH589 (Figure 3B). Other non-selective HDAC inhibitors (TSA, SAHA) also downregulated p-STAT3 (Figure 3C). To determine whether downregulation of p-STAT3

induced by non-selective HDAC inhibitors is mediated via HDAC3 inhibition, we next examined p-STAT3 in HDAC3 knockdown MM cells. Both tyrosine (Y705) and serine (S727) phosphorylation of STAT3 were markedly downregulated in HDAC3 knockdown cells, without inhibition of p-ERK (Figure 3D). Importantly, no downregulation of p(Y705)-STAT3 was observed in HDAC1 or HDAC2 knockdown cells (Figure 3E), further confirming that HDAC3 specifically modulates STAT3 phosphorylation in MM cells.

Since STAT3 can be acetylated at lysine 685 [19], we next examined whether HDAC3 knockdown affects STAT3 acetylation. As shown in Figure 3F (left panel), STAT3 was hyperacetylated in HDAC3 knockdown RPMI8226 cells; however, the cross-talk between STAT3 phosphorylation and acetylation remains unclear. Interestingly, phosphorylation of JAK2, an upstream molecule of STAT3, was upregulated in HDAC3 knockdown cells (Figure 3F, right panel), suggesting a possible positive feedback loop associated with downregulated p-STAT3. These results suggest that HDAC3 knockdown directly inhibits phosphorylation on both Y705 and S727 of STAT3.

HDAC3 selective inhibitor triggers significant MM cell growth inhibition

To both further validate the role of HDAC3 in MM biology and provide the framework for derived clinical trials targeting HDAC3, we have recently produced and validated the ortho-amino anilide BG45 to be an HDAC class I inhibitor with selectivity for HDAC3 (IC50 = 289nM) over HDAC1, 2 (Supplemental Figure 2B, Table 1) [12]. Consistent with HDAC3 knockdown data above, BG45 significantly inhibited MM cell growth in a dose-dependent fashion, as assessed by MTT assay (Figure 4A). Importantly, BG45 also triggered a potent growth inhibitory effect against patient-derived MM cells (Figure 4B), without affecting normal donor PBMCs (Figure 4C). These results suggest that BG45 selectively targets MM cells. We next examined whether BG45 overcomes the anti-apoptotic effect of BMSCs [20]: importantly, BG45 in a dose-dependent fashion markedly inhibited MM cell growth even in the presence of BMSCs (Figure 4D), associated with caspase-3/PARP cleavage (Figure 4E). These results suggest BG45 induces caspase-dependent apoptosis in MM cells.

We further assessed the mechanism of the HDAC inhibitory effect by BG45 by profiling its effect on histone acetylation in MM cells. BG45 in a dose-dependent fashion significantly induced acetylation of histone H2A, H3, and H4 in MM.1S cells (Figure 4F, left panel). In contrast, BG45 treatment did not increase α-tubulin acetylation, a biomarker of HDAC6 inhibition (Figure 4F, right panel), further indicating its selectivity against HDAC3. In contrast, the non-selective HDAC inhibitor LBH589 significantly triggered both histone and α-tubulin acetylation. We next examined the impact of BG45 on STAT3 phosphorylation in MM.1S cells. Consistent with the results obtained for HDAC3 knockdown, BG45 in a dose-dependent fashion markedly downregulated p-STAT3, without affecting p-ERK1/2 (Figure 4G). Importantly, we also observed that BG45 increased acetylation of STAT3 in MM.1S cells (Figure 4H). Taken together, these results demonstrate that the HDAC3 selective inhibitor BG45-induced MM cell toxicity is associated with hyperacetylation of histones and STAT3, as well as downregulation of p-STAT3.

HDAC3 inhibition synergistically enhances bortezomib-induced cytotoxicity

Non-selective HDAC inhibitors show only modest anti-MM activities as single agents, which can be markedly enhanced in combination with bortezomib [6, 7]. We have also shown that HDAC6 selective inhibitors tubacin and ACY1215 synergistically augment bortezomib-induced cytotoxicity due to dual blockade of proteasomal and aggresomal protein degradation, evidenced by accumulation of ubiquitinated proteins [6, 7]. However, the mechanism underlying the synergistic effect of bortezomib combined with class-I HDAC inhibitors has not yet been defined. We therefore next examined combination treatment of RPMI8226 cells with bortezomib and either Merck60 or MS275. Importantly, we observed synergistic cytotoxicity triggered by bortezomib in combination with MS275, but not with Merck60 (Figure 5A and Table 2). Moreover, bortezomib significantly enhances cytotoxicity in HDAC3 knockdown cells (Figure 5B), indicating that HDAC3 has a key role in mediating the synergistic anti-MM activity induced by class-I HDAC inhibitors with bortezomib. We have previously shown that bortezomib upregulates Akt activity, which can be inhibited by Akt inhibitor perifosine, and that combined therapy with bortezomib and perifosine tiggers synergistic cytotoxicity in MM cells [9]. Since previous studies have shown that bortezomib upregulates activated STAT3 in head and neck squamous cell carcinoma [21], we here similarly examined whether bortezomib enhances p-STAT3 in MM cells. Importantly, we observed that bortezomib upregulated p-STAT3, which is completely abrogated in HDAC3, but not in HDAC1 or HDAC2, knockdown cells (Figure 5C). These results suggest that the synergistic cytotoxicity induced by combined HDAC3 knockdown with bortezomib is mediated, at least in part, by inhibition of STAT3 activity.

We similarly evaluated the combination effect of bortezomib with selective HDAC3 inhibitor BG45. Of note, BG45 did not inhibit HDAC6 evidenced by hyperacetylation of α-tubulin (Supplementary Figure 3A). Consistent with HDAC3 knockdown data, BG45 in a dose-dependent fashion also synergistically enhanced bortezomib-induced cytotoxicity (Figure 5D, Table 2C). We also examined whether dual inhibition of both HDAC3 and HDAC6 was more cytotoxic than either HDAC3 or HDAC6 when combined with bortezomib. As expected, HDAC6 selective inhibitor tubastatin-A further enhanced cytotoxicity induced by combined HDAC3 knockdown with bortezomib (Supplementary Figure 3B).

BG45 demonstrate significant anti-MM activities in a murine xenograft model

To evaluate the in vivo impact of BG45 alone or in combination with bortezomib, we used the subcutaneous MM.1S xenograft model of human MM in mice. BG45 significantly inhibited MM tumor growth in the treatment versus control group in a dose-dependent fashion. For example, significant differences were observed in control versus BG45 15 mg/kg, control versus BG45 50 mg/kg, and BG45 15 mg/kg versus BG45 50 mg/kg at day 22 ($p < 0.05$, Figure 6A). Moreover, BG45 50 mg/kg in combination with bortezomib further enhanced either single agent activity ($p < 0.01$). Representative images of tumor growth inhibition by BG45 (50 mg/kg) are demonstrated in Figure 6B. These results confirmed that BG45 triggers in vivo anti-MM activities.

Discussion

Histone deacetylases regulate the activity of tumor-suppressor genes and oncogenes that play pivotal roles in tumorigenesis [22] and have been investigated in preclinical studies in both solid tumors and hematologic malignancies, including MM [4, 23]. However, the clinical utility of these agents is limited due to unfavorable toxicities attendant to non-selective HDAC inhibition. Indeed, non-selective HDAC inhibitors show different inhibitory profiles of class-I to class-IV DACs [12]. To date, however, the biologic impact of isoform-selective HDAC inhibitors on MM cell growth and/or survival has not yet been elucidated. Interestingly, previous studies have shown that selective inhibition of HDAC1, 2 by Merck60 treatment triggers significant growth inhibition in B-cell acute lymphocytic leukemia cells [24]. We here observed that MS275 (HDAC1, 2, 3 inhibition) induces significantly greater MM cell growth inhibition than Merck60 (HDAC1, 2 inhibition), and demonstrate the biologic impact of HDAC3 inhibition on MM cell growth and survival in the context of the BM microenvironment using combined genetic and pharmacological probes.

We examined the biologic impact of HDAC3 in MM cells using HDAC3 knockdown and HDAC3-selective small molecule inhibitor BG45. Both induce significant growth inhibition in MM cell lines and patient MM cells, without toxicity in PBMCs. In contrast, modest or no growth inhibitory effect of HDAC1 or HDAC2 knockdown was recognized. Consistent with our previous studies using non-selective HDAC inhibitors (ie, SAHA, LAQ824, LBH589) [25–27], the MM cell growth inhibitory effect induced by either HDAC3 knockdown or BG45 is associated with markedly increased $p21^{WAF1}$, followed by apoptosis evidenced by cleavage of caspases and PARP. Taken together, these results strongly suggest that class-I HDAC inhibitor- or non-selective HDAC inhibitor-induced MM cell growth inhibition is due to HDAC3 inhibition. They further suggest that more selective HDAC3 inhibitor may have a more favorable side effect profile than class-I or non-selective HDAC inhibitors.

We have previously shown that both non-selective HDAC inhibitors and HDAC6-selective inhibitors tubacin and ACY-1215 significantly enhance bortezomib-induced cytotoxicity in MM cells, associated with dual proteasome and aggresome blockade [6, 7]. Since non-selective HDAC inhibitors can block both class-I (HDAC1, 2, 3 and 8) and class-IIb (HDAC6, 10), we next determined whether the enhanced cytotoxicity of bortezomib combined with non-selective HDAC inhibitors is due solely to HDAC6 inhibition, or also to class-I HDAC blockade. Importantly, MS275, but not Merck60, augments bortezomib-induced cytotoxicity in MM cells. Moreover, both HDAC3 knockdown and BG45 similarly significantly enhance bortezomib-induced cytotoxicity, confirming the pivotal role of HDAC3 blockade in mediating enhanced cytotoxicity in combination with bortezomib. Bortezomib with HDAC6 inhibitors achieves dual inhibition of proteasomal and aggresomal protein degradation and accumulation of polyubiquitinated proteins [6, 7], which was not observed by bortezomib and HDAC3 knockdown. Therefore differential mechanisms of action of HDAC3 (class-I) versus HDAC6 (class-IIb) inhibition mediate enhanced bortezomib-induced cytotoxicity in MM cells.

We have shown that the BM microenvironment induces MM cell proliferation, survival, drug resistance, and migration [20, 28]. The JAK2/STAT3 pathway mediates MM cell survival by regulating anti-apoptotic proteins including Mcl-1, Bcl-xL, and survivin [17, 29–31]; therefore, inhibition of JAK2/STAT3 pathway is a potential therapeutic target. Indeed, we and others have shown that STAT3 inhibition by RNAi or small molecule inhibitors significantly inhibits MM cell growth [15, 17, 32]. Importantly, we here found that HDAC3 knockdown markedly decreases both tyrosine (Y705) and serine (S727) phosphorylation of STAT3. Moreover, either HDAC3 knockdown or BG45 inhibit p-STAT3 and MM cell growth, even in the presence of exogenous IL-6 or BMSC culture supernatants.

Previous studies have shown that STAT3 acetylation is regulated by HDAC3 in multiple cancers [14, 19, 33], indicating that STAT3 is one of non-histone substrate proteins were hyperacetylated by HDAC3 inhibition. We therefore examined the impact of HDAC3 inhibition on STAT3 acetylation. Consistent with previous studies, we observed that acetylation of STAT3 in MM cells is upregulated by both HDAC3 knockdown and BG45. Since HDAC3 knockdown or inhibition triggers both upregulation of acetylation and downregulation of phosphorylation of STAT3, these results suggest crosstalk signaling, and that hyperacetylation may inhibit phosphorylation of STAT3. Previous studies have also shown that HDAC3 knockdown upregulates acetylation of STAT3 and downregulates pSTAT3 in diffuse large B-cell lymphoma cells [14]; however, the precise is unknown and the object of our ongoing studies. Importantly HDAC6 inhibition enhances cytotoxicity induced by HDAC3 knockdown with bortezomib, further suggesting differential mechanisms of action whereby HDAC6 inhibition versus HDAC3 inhibition enhances bortezomib-induced cytotoxicity.

In summary, we demonstrated remarkable growth inhibitory effect of BG45, alone and in combination, in a murine xenograft model of human MM cells. Our results therefore demonstrate the role of HDAC3 in MM cell growth in the BM microenvironment and provide the preclinical rationale for targeting HDAC3, alone and in combination with proteasome inhibitors, to improve patient outcome in MM.

Supplementary Material

Refer to Web version on PubMed Central for supplementary material.

Acknowledgments

This study was supported by the National Institute of Health Grants (SPORE-P50100707, P01 CA78378, R01 CA50947 (K.C.A.), R01 DA02830 (S.J.H.) and P50CA086355 (R.M.)). K.C.A. is an American Cancer Society Clinical Research Professor.

References

1. Quintas-Cardama A, Santos FP, Garcia-Manero G. Histone deacetylase inhibitors for the treatment of myelodysplastic syndrome and acute myeloid leukemia. Leukemia. 2011; 25:226–235. [PubMed: 21116282]
2. Deangelo DJ, Spencer A, Bhalla KN, Prince HM, Fischer T, Kindler T, et al. Phase Ia/II, two-arm, open-label, dose-escalation study of oral panobinostat administered via two dosing schedules in patients with advanced hematologic malignancies. Leukemia. 2013 in press.

3. Zhang QL, Wang L, Zhang YW, Jiang XX, Yang F, Wu WL, et al. The proteasome inhibitor bortezomib interacts synergistically with the histone deacetylase inhibitor suberoylanilide hydroxamic acid to induce T-leukemia/lymphoma cells apoptosis. Leukemia. 2009; 23:1507–1514. [PubMed: 19282831]
4. Lane AA, Chabner BA. Histone deacetylase inhibitors in cancer therapy. J Clin Oncol. 2009; 27:5459–5468. [PubMed: 19826124]
5. Dimopoulos M, Jagannath S, Yoon S-S, Siegel D, Lonial S, Hajek R, et al. Vantage 088. Vorinostst in combination with bortezomib in patients with relapsed refractory multiple myeloma: results of a global randomized phase 3 trial. Blood. 2011; 118:368–369. [PubMed: 21586752]
6. Hideshima T, Bradner JE, Wong J, Chauhan D, Richardson P, Schreiber SL, et al. Small-molecule inhibition of proteasome and aggresome function induces synergistic antitumor activity in multiple myeloma. Proc Natl Acad Sci U S A. 2005; 102:8567–8572. [PubMed: 15937109]
7. Santo L, Hideshima T, Kung AL, Tseng JC, Tamang D, Yang M, et al. Preclinical activity, pharmacodynamic, and pharmacokinetic properties of a selective HDAC6 inhibitor, ACY-1215, in combination with bortezomib in multiple myeloma. Blood. 2012; 119:2579–2589. [PubMed: 22262760]
8. Raje N, Mahindra A, Vogl D, Voorhees P, W B, Hari P, et al. New drug partner for combination therapy in multiple myeloma (MM): development of ACY-1215, a selective histone deacetylase 6 inhibitor alone and in combination with bortezomib or lenalidomide. Haematologica. 2013; 98(S1): 320.
9. Hideshima T, Catley L, Yasui H, Ishitsuka K, Raje N, Mitsiades C, et al. Perifosine, an oral bioactive novel alkylphospholipid, inhibits Akt and induces in vitro and in vivo cytotoxicity in human multiple myeloma cells. Blood. 2006; 107:4053–4062. [PubMed: 16418332]
10. Cirstea D, Hideshima T, Santo L, Eda H, Mishima Y, Nemani N, et al. Small molecule Multi-Targeted kinase inhibitor RGB-286638 Triggers P53-Dependent and -Independent Anti-Multiple myeloma activity through inhibition of transcriptional CDKs. Leukemia. 2013 in press.
11. Tai YT, Landesman Y, Acharya C, Calle Y, Zhong MY, Cea M, et al. CRM1 inhibition induces tumor cell cytotoxicity and impairs osteoclastogenesis in multiple myeloma: molecular mechanisms and therapeutic implications. Leukemia. 2013 in press.
12. Bradner JE, West N, Grachan ML, Greenberg EF, Haggarty SJ, Warnow T, et al. Chemical phylogenetics of histone deacetylases. Nat Chem Biol. 2010; 6:238–243. [PubMed: 20139990]
13. Togi S, Kamitani S, Kawakami S, Ikeda O, Muromoto R, Nanbo A, et al. HDAC3 influences phosphorylation of STAT3 at serine 727 by interacting with PP2A. Biochem Biophys Res Commun. 2009; 379:616–620. [PubMed: 19121623]
14. Gupta M, Han JJ, Stenson M, Wellik L, Witzig TE. Regulation of STAT3 by histone deacetylase-3 in diffuse large B-cell lymphoma: implications for therapy. Leukemia. 2012; 26:1356–1364. [PubMed: 22116549]
15. Santo L, Hideshima T, Cirstea D, Bandi M, Nelson EA, Gorgun G, et al. Antimyeloma activity of a multitargeted kinase inhibitor, AT9283, via potent Aurora kinase and STAT3 inhibition either alone or in combination with lenalidomide. Clin Cancer Res. 2011; 17:3259–3271. [PubMed: 21430070]
16. Hideshima T, Mitsiades C, Ikeda H, Chauhan D, Raje N, Gorgun G, et al. A proto-oncogene BCL6 is up-regulated in the bone marrow microenvironment in multiple myeloma cells. Blood. 2010; 115:3772–3775. [PubMed: 20228272]
17. Nelson EA, Walker SR, Kepich A, Gashin LB, Hideshima T, Ikeda H, et al. Nifuroxazide inhibits survival of multiple myeloma cells by directly inhibiting STAT3. Blood. 2008; 112:5095–5102. [PubMed: 18824601]
18. Hideshima T, Chauhan D, Hayashi T, Akiyama M, Mitsiades N, Mitsiades C, et al. Proteasome inhibitor PS-341 abrogates IL-6 triggered signaling cascades via caspase-dependent downregulation of gp130 in multiple myeloma. Oncogene. 2003; 22:8386–8393. [PubMed: 14627979]
19. Yuan ZL, Guan YJ, Chatterjee D, Chin YE. Stat3 dimerization regulated by reversible acetylation of a single lysine residue. Science. 2005; 307:269–273. [PubMed: 15653507]

20. Hideshima T, Anderson KC. Molecular mechanisms of novel therapeutic approaches for multiple myeloma. Nat Rev Cancer. 2002; 2:927–937. [PubMed: 12459731]
21. Li C, Zang Y, Sen M, Leeman-Neill RJ, Man DS, Grandis JR, et al. Bortezomib up-regulates activated signal transducer and activator of transcription-3 and synergizes with inhibitors of signal transducer and activator of transcription-3 to promote head and neck squamous cell carcinoma cell death. Mol Cancer Ther. 2009; 8:2211–2220. [PubMed: 19638453]
22. Singh BN, Zhang G, Hwa YL, Li J, Dowdy SC, Jiang SW. Nonhistone protein acetylation as cancer therapy targets. Expert Rev Anticancer Ther. 2010; 10:935–954. [PubMed: 20553216]
23. Schrump DS. Cytotoxicity mediated by histone deacetylase inhibitors in cancer cells: mechanisms and potential clinical implications. Clin Cancer Res. 2009; 15:3947–3957. [PubMed: 19509170]
24. Stubbs MC, Kim WI, Davis T, Qi J, Bradner J, Kung AL, et al. Selective inhibition of HDAC1 and HDAC2 Is a potential therapeutic option for B-ALL. Blood. 2010; 116:1194–1194. [PubMed: 20798242]
25. Mitsiades N, Mitsiades CS, Richardson PG, McMullan C, Poulaki V, Fanourakis G, et al. Molecular sequelae of histone deacetylase inhibition in human malignant B cells. Blood. 2003; 101:4055–4062. [PubMed: 12531799]
26. Catley L, Weisberg E, Tai YT, Atadja P, Remiszewski S, Hideshima T, et al. NVP-LAQ824 is a potent novel histone deacetylase inhibitor with significant activity against multiple myeloma. Blood. 2003; 102:2615–2622. [PubMed: 12816865]
27. Catley L, Weisberg E, Kiziltepe T, Tai YT, Hideshima T, Neri P, et al. Aggresome induction by proteasome inhibitor bortezomib and alpha-tubulin hyperacetylation by tubulin deacetylase (TDAC) inhibitor LBH589 are synergistic in myeloma cells. Blood. 2006; 108:3441–3449. [PubMed: 16728695]
28. Hideshima T, Mitsiades C, Tonon G, Richardson PG, Anderson KC. Understanding multiple myeloma pathogenesis in the bone marrow to identify new therapeutic targets. Nat Rev Cancer. 2007; 7:585–598. [PubMed: 17646864]
29. Raje N, Kumar S, Hideshima T, Roccaro A, Ishitsuka K, Yasui H, et al. Seliciclib (CYC202 or R-roscovitine), a small-molecule cyclin-dependent kinase inhibitor, mediates activity via down-regulation of Mcl-1 in multiple myeloma. Blood. 2005; 106:1042–1047. [PubMed: 15827128]
30. Alas S, Bonavida B. Inhibition of constitutive STAT3 activity sensitizes resistant non-Hodgkin's lymphoma and multiple myeloma to chemotherapeutic drug-mediated apoptosis. Clin Cancer Res. 2003; 9:316–326. [PubMed: 12538484]
31. Bhutani M, Pathak AK, Nair AS, Kunnumakkara AB, Guha S, Sethi G, et al. Capsaicin is a novel blocker of constitutive and interleukin-6-inducible STAT3 activation. Clin Cancer Res. 2007; 13:3024–3032. [PubMed: 17505005]
32. Burger R, Le Gouill S, Tai YT, Shringarpure R, Tassone P, Neri P, et al. Janus kinase inhibitor INCB20 has antiproliferative and apoptotic effects on human myeloma cells in vitro and in vivo. Mol Cancer Ther. 2009; 8:26–35. [PubMed: 19139110]
33. Lee JL, Wang MJ, Chen JY. Acetylation and activation of STAT3 mediated by nuclear translocation of CD44. J Cell Biol. 2009; 185:949–957. [PubMed: 19506034]

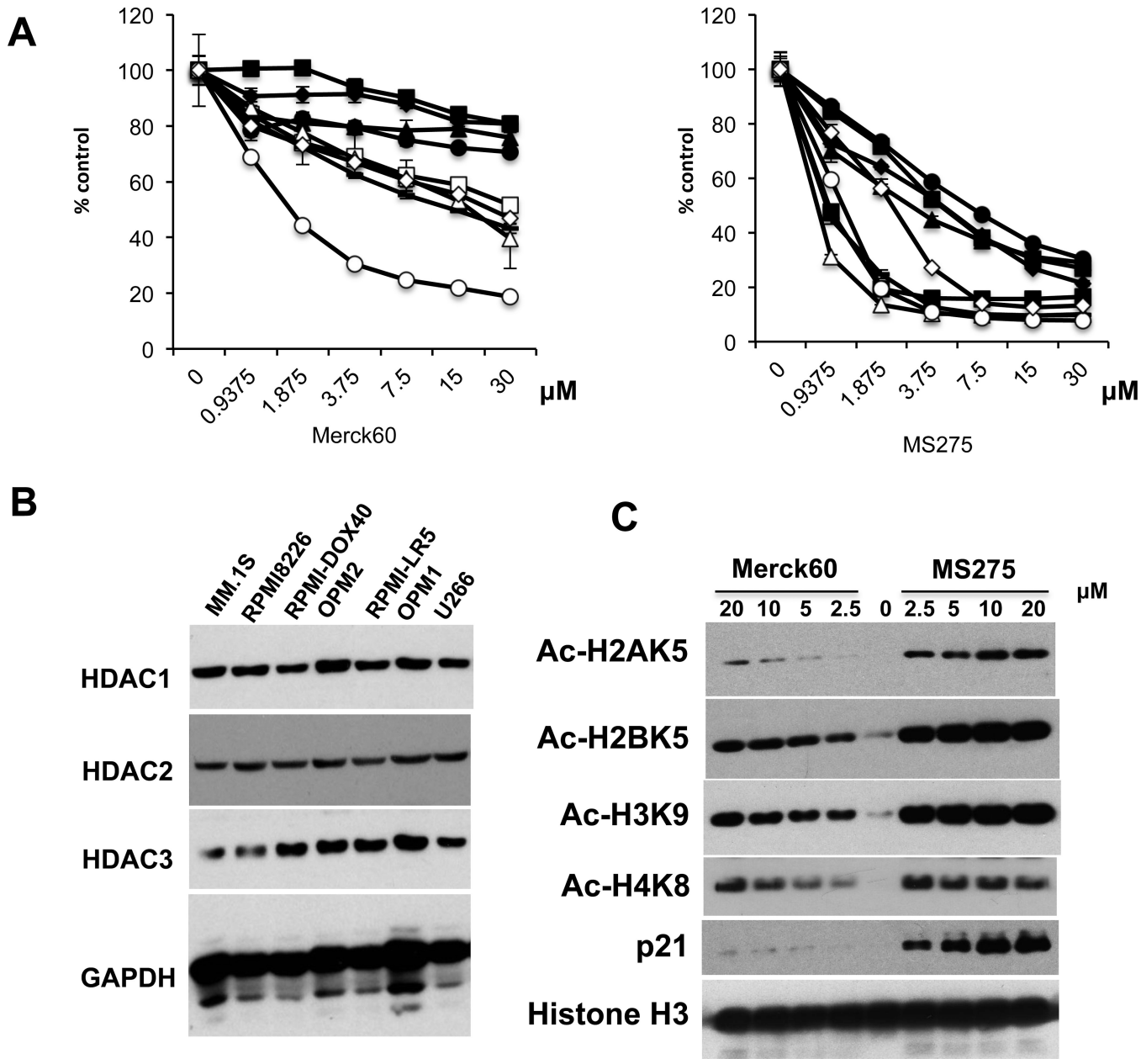

Figure 1. MS275 is more cytotoxic than Merck60 in MM cells

(A) MM.1S (□), RPMI8226 (●), U266 (▲), H929 (■), MM.1R (Δ), RPMI-LR5 (♦), OPM1 (−), OPM2 (○), RPMI-DOX40 (◊) MM cells were cultured with Merck60 (left panel) or MS275 (right panel) for 48 hours. Cell growth was assessed by MTT assay. All experiments were performed 3 times in quadruplicate. Data represent mean ± SD. (B) Whole cell lysates from MM cells lines were subjected to immunoblotting to assess HDAC1, 2 and 3 expression. GAPDH served as a loading control. (C) Whole cell lysates from RPMI8226 cells treated with Merck60 or MS275 for 12h were subjected to immunoblotting with anti-Ac-H2AK5, -Ac-H2BK5, -Ac-H3K9, -Ac-H4K8, -p21^{WAF1}. and -histone H3 antibodies (Abs).

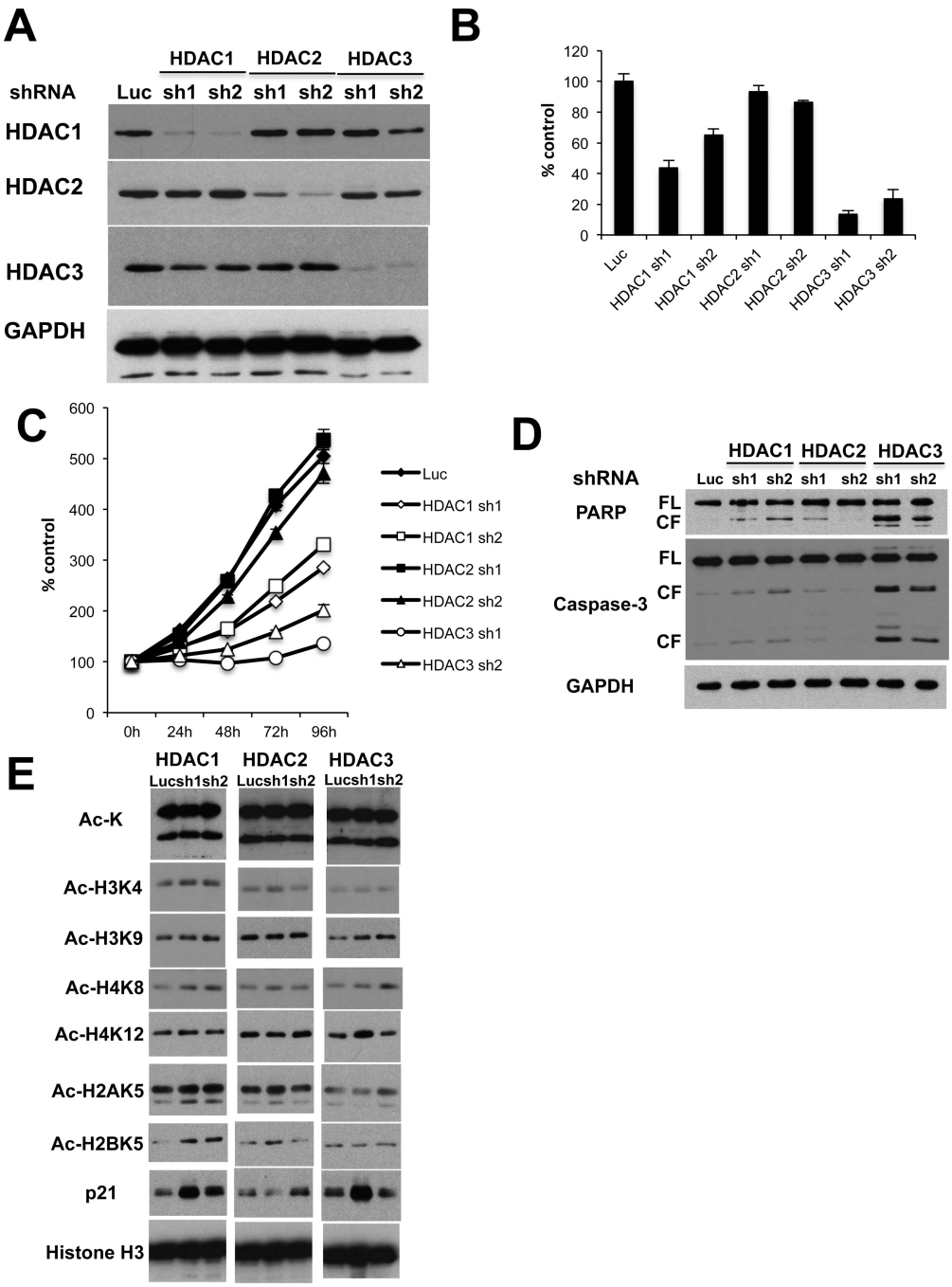

Figure 2. HDAC3 knockdown inhibits MM cell growth

RPMI8226 cells were infected with either luciferase (Luc, as control), HDAC1 (sh1, sh2), HDAC2 (sh1, sh2) or HDAC3 (sh1 or sh2) shRNAs. (A) Whole cell lysates were subjected to western blotting with anti-HDAC1, -HDAC2, -HDAC3 and -GAPDH Abs. (B) Cell proliferation was assessed by DNA synthesis using ^{3}[H]-thymidine uptake. All experiments were performed 3 times in quadruplicate. Data represent mean ± SD. (C) Infected cells were cultured for indicated time periods, and cell growth was assessed by MTT assay. All experiments were performed 3 times in quadruplicate. Data represent mean ± SD. (D)

Whole cell lysates were subjected to immunoblotting with anti-caspase-3, -PARP, and -GAPDH Abs. FL and CF indicate full-length and cleaved form, respectively. (E) Whole cell lysates were subjected to immunoblotting with anti-Ac-K, -Ac-H3K4, -Ac-H3K9, -Ac-H4K8, -Ac-H4K12, -Ac-H2AK5, -Ac-H2BK5 and -histone H3 Abs.

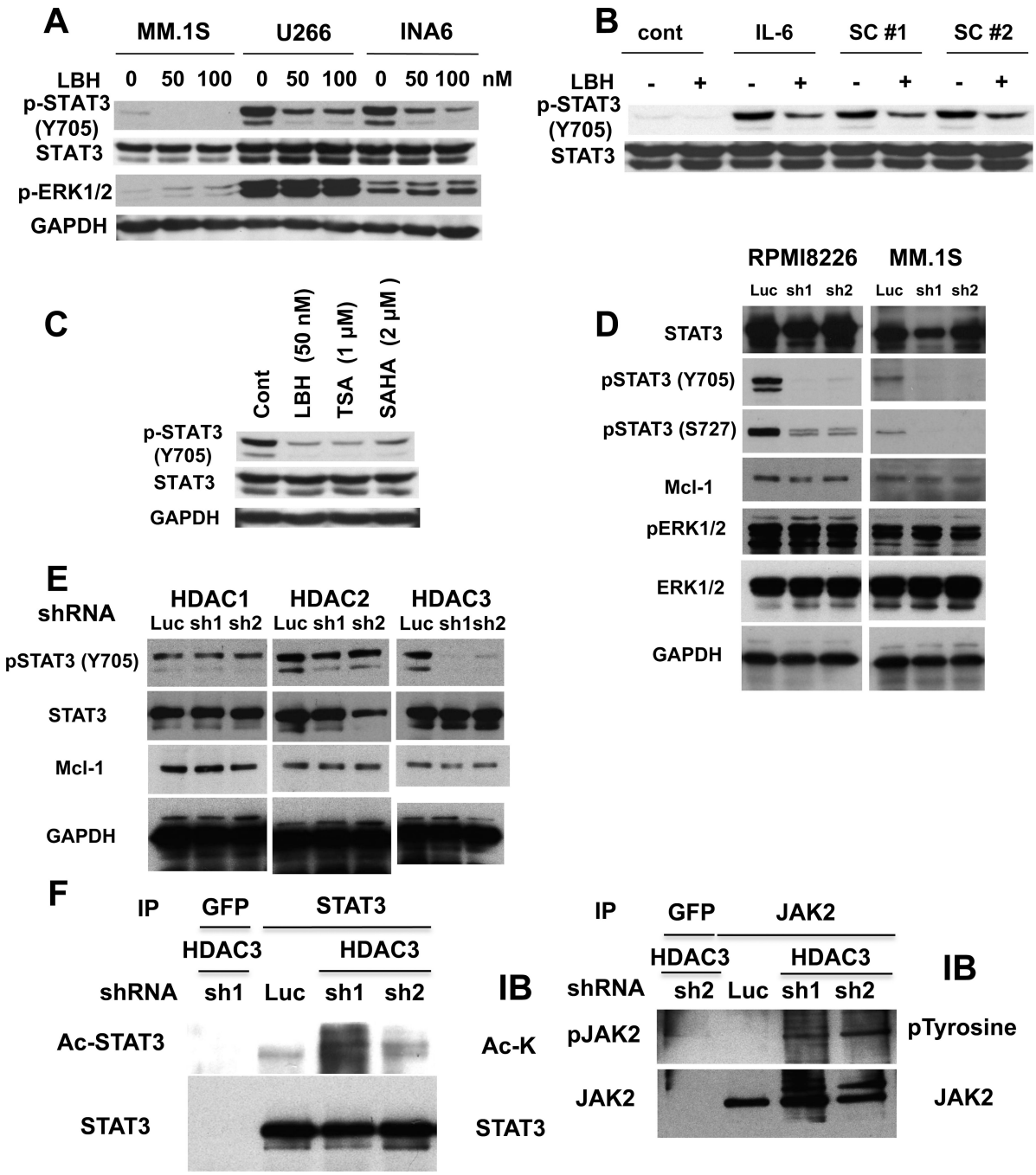

Figure 3. Downregulation of HDAC3 inhibits p-STAT3

(A) MM.1S, U266, and INA6 cells were cultured with DMSO control or LBH589 (50 and 100 nM) for 8h. Whole cell lysates were subjected to immunoblotting with anti-STAT3, -pSTAT3 (Tyr705), -pERK1/2, and -GAPDH Abs. (B) MM.1S cells pretreated with or without 50 nM LBH589 for 8 hours were then treated with IL-6 (10 ng/mL) or BMSC culture supernatants (#1 and #2) for 15 mimutes. Whole cell lysates were subjected to immunoblotting with anti-pSTAT3 (Tyr705) and STAT3 Abs. (C) INA-6 cells were cultured with DMSO control, LBH589 (50 nM), TSA (1 μM) or SAHA (2 μM) for 8 hours.

Whole cell lysates were subjected to immunoblotting with anti-pSTAT3 (Tyr705), STAT3, and GAPDH Abs. (D) RPMI8226 (left panel) and MM.1S (right panel) cells were infected with either Luc or HDAC3 (#1 and #2) shRNAs. Whole cell lysates were subjected to immunoblotting with anti-STAT3, -pSTAT3 (Tyr705), -pSTAT3 (Ser727), -pERK1/2, -ERK1/2, and -GAPDH Abs. (E) RPMI8226 cells were infected with Luc or HDAC1 (#1 and #2), HDAC2 (#1 and #2) or HDAC3 (#1 and #2) shRNAs. Whole cell lysates were subjected to immunoblotting with anti-pSTAT3 (Tyr705), -STAT3 and -GAPDH Abs. (F) and (G) RPMI8226 cells were infected with either Luc or HDAC3 (#1 and #2) shRNAs. Whole cell lysates were immunoprecipitated with (F) anti-GFP or -STAT3 or (G) -JAK2 Abs. Immunoprecipitates were subjected to SDS-PAGE and immunoblotted with (F) Ac-lysine and STAT3 or (G) p-tyrosine and JAK2.Abs

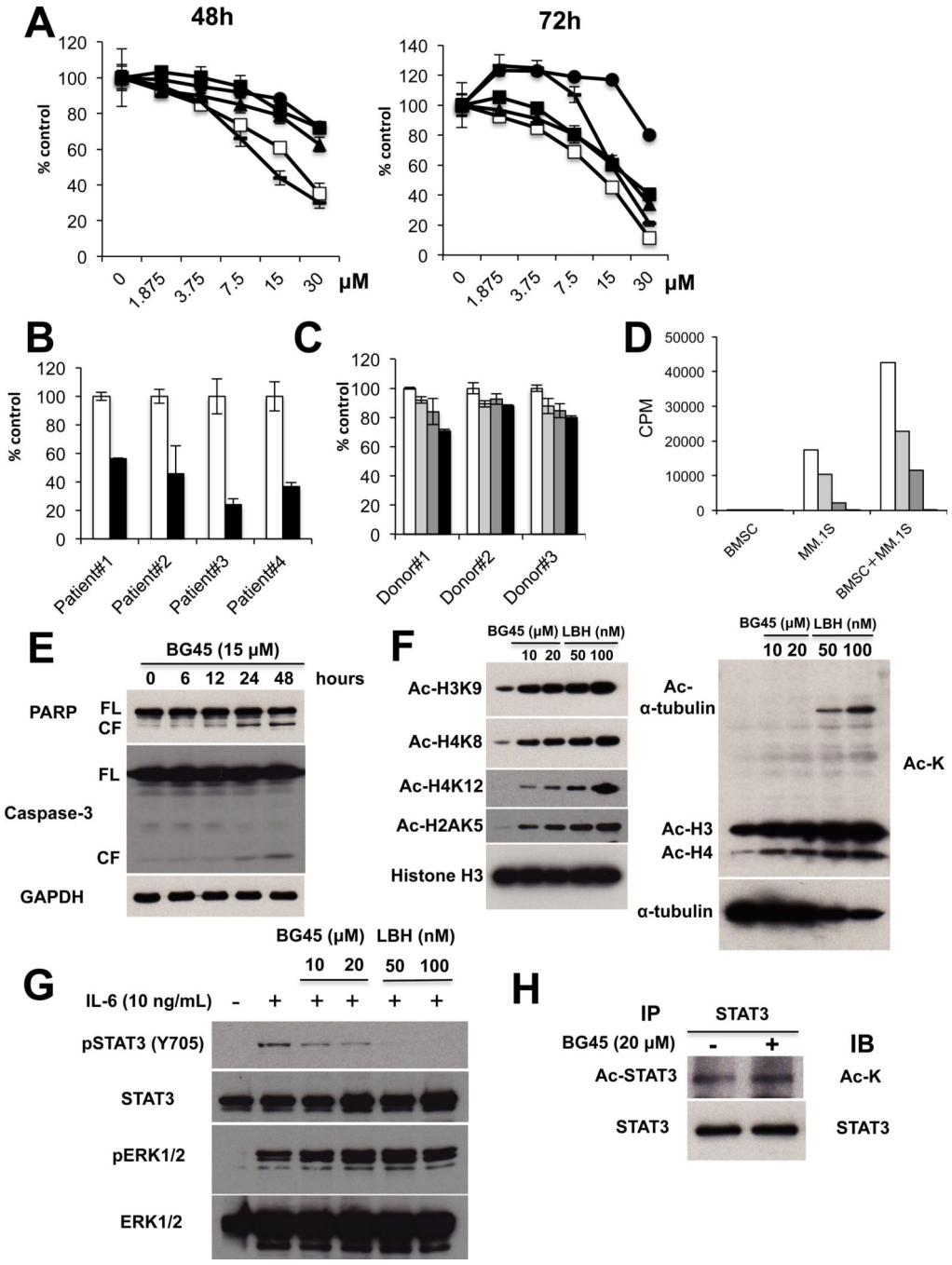

Figure 4. HDAC3 selective inhibitor triggers significant MM cell growth inhibition

(A) MM.1S (□), RPMI8226 (●), U266 (▲), OPM1 (−), and H929 (■) MM cells were cultured with or without BG45 (1.875 – 30 μM) for 48h (left panel) and 72h (right panel). Cell growth was assessed by MTT assay. All experiments were performed 3 times in quadruplicate. Data represent mean ± SD. (B) Primary tumor cells from MM patients were treated with (30 μM, ■) or without (□) BG45 for 72 hours. Cell growth was then assessed by MTT assay. Data represents mean ± SD from triplicates cultures. (C) PBMCs were cultured with 0 μM (□), 7.5 μM (▒), 15 μM (▓) or 30 μM (■) BG45 for 72 hours. Cell

growth was assessed by MTT assay. The data represents mean ± SD from triplicate cultures. (D) MM.1S cells co-cultured with BMSCs were treated with 0 μM (□), 7.5 μM (▒), 15 μM (▓) or 30 μM (■) BG45 for 48 hours. Cell proliferation was measured by 3[H]-thymidine incorporation assay. Data represent mean ± SD from quadruplicate cultures. (E) MM.1S cells were cultured with or without BG45 (15 μM) for the indicated time periods. Whole cell lysates were subjected to immunoblotting with anti-Caspase-3, -PARP and -GAPDH Abs. FL and CF indicate full-length and cleaved forms, respectively. (F) MM.1S cells were cultured with BG45 (10 and 20 μM) or LBH589 (50 and 100 nM) for 12h. Whole cell lysates were then subjected to immunoblotting with anti-Ac-H3K9, -Ac-H4K8, -Ac-H4K12, -Ac-H2AK5, -and Ac-H3 Abs (left panel), as well as Ac-lysine and Ac-α-tubulin Abs (right panel). (G) MM.1S cells were cultured with or without BG45 (10 and 20 μM) or LBH589 (50 and 100 nM) for 10 hours and then stimulated with IL-6 (10 ng/mL) for 4 hours. Whole cell lysates were subjected to immunoblotting with anti-pSTAT3 (Tyr705), -STAT3, -pERK1/2 (Thr202/204), and -ERK1/2 Abs. (H) MM.1S cells were treated with or without BG45 (20 μM) for 18 hours. Whole cell lysates were immunoprecipitated with anti-STAT3 Ab. Immunoprecipitaes were then subjected to SDS-PAGE and immunoblotted with anti -Ac-K and -STAT3 Abs.

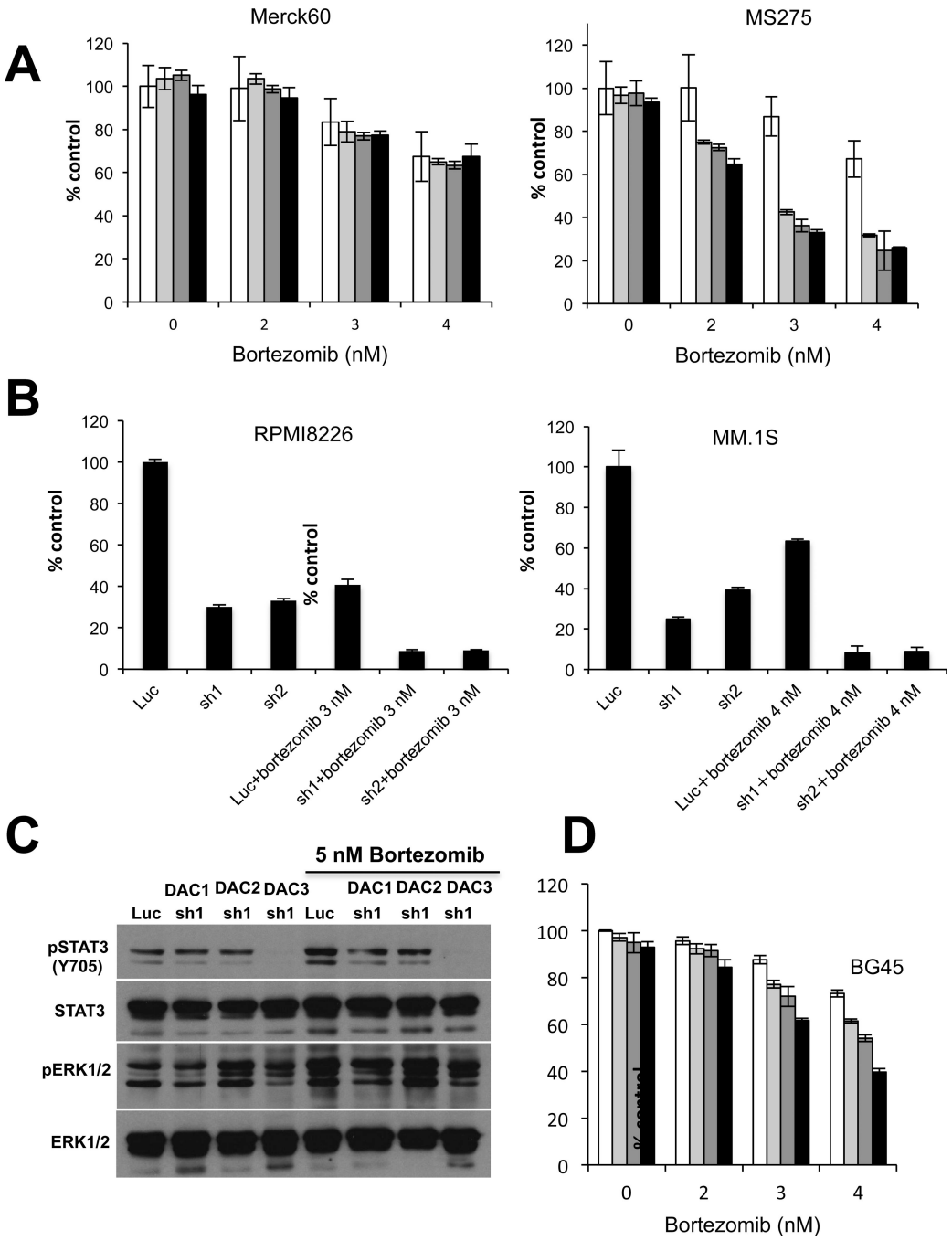

Figure 5. HDAC3 inhibition enhances bortezomib-induced cytotoxicity

(A) RPMI8226 cells were treated with bortezomib (0 – 4 nM) in combination with 0 μM (□), 1 μM (□), 2 μM (▒) or 3 μM (■) Merck60 (left panel) or MS275 (right panel) for 24 hours. (B) RPMI8226 (left panel) and MM.1S (right panel) cells were infected with Luc or HDAC3 (#1 and #2) shRNAs. Cells were then cultured with or without bortezomib (3 nM) for 48 hours and cell growth was assessed by MTT assay. Data represent mean ± SD from triplicate cultures. (C) RPMI8226 cells were infected with Luc, HDAC1 (sh1), HDAC2 (sh1) or HDAC3 (sh1) shRNAs and then treated with or without bortezomib (5 nM) for 6

hours. Whole cell lysates were subjected to immunoblotting with anti-STAT3, -pSTAT3 (Tyr705), -pERK1/2 (Thr202/204) and -ERK1/2 Abs. (D) RPMI8226 cells were treated with bortezomib (2 – 4 nM) in the presence of 0 μM (□), 5 μM (▫), 10 μM (▪) or 20 μM (■) BG45 for 24h, and cell growth was then assessed by MTT assay. All experiments were performed 3 times in quadruplicate. Data represent mean ± SD.

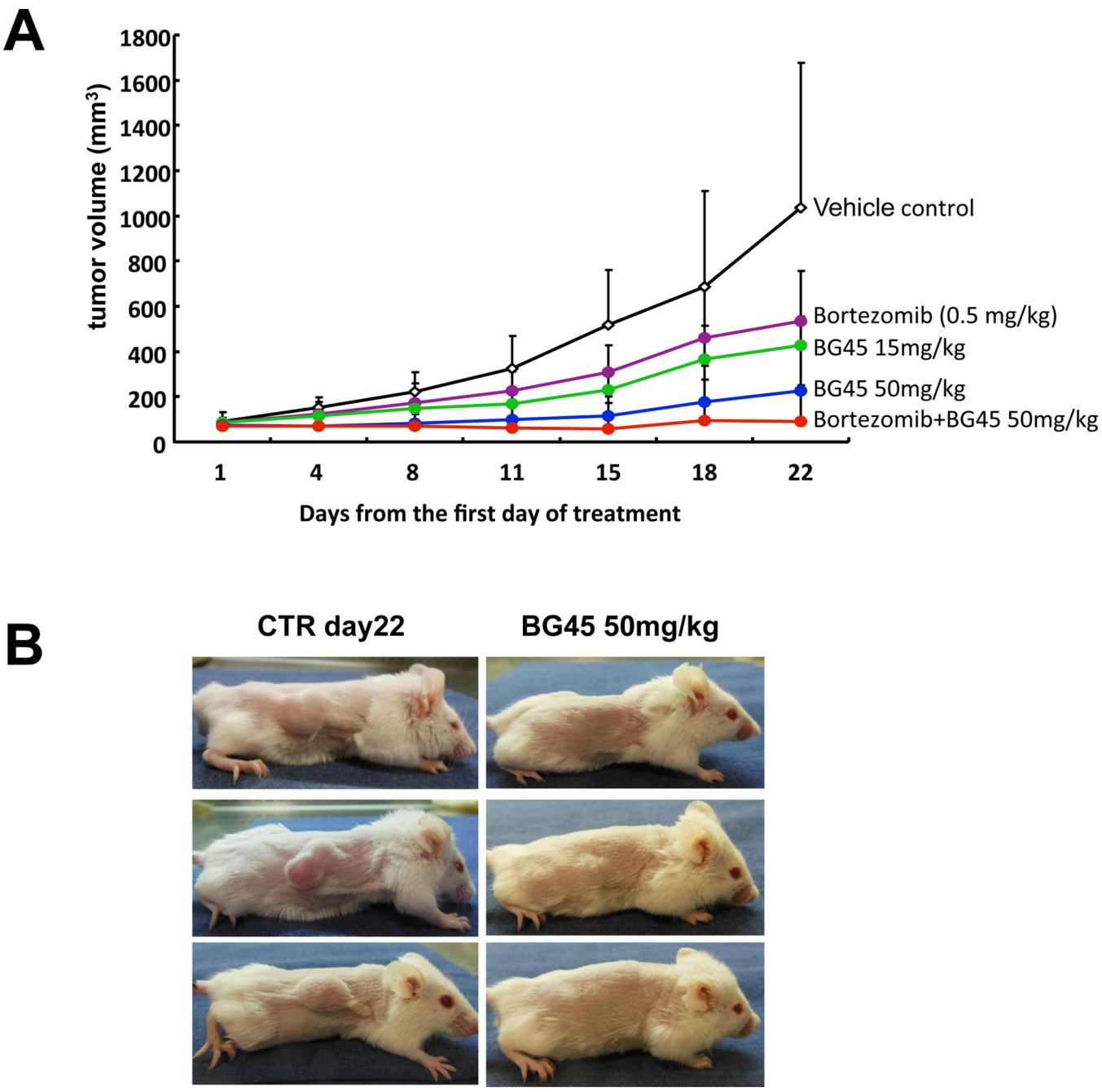

Figure 6. BG45 inhibits human MM cell growth and enhances bortezomib-induced cytotoxicity in vivo

SCID mice were subcutaneously injected 5×10^6 MM.1S cells. After development of measurable tumors, cohorts were treated for 3 weeks with vehicle control (black line), 15 mg/kg BG45 (green line), 50 mg/kg BG45 (blue line), 0.5 mg bortezomib (purple line), or 50 mg/kg BG45 with bortezomib (red line) for 3 weeks. (A) Tumor volume was calculated from caliper measurements twice weekly, and data represent mean ± SD. (B) Representative

whole-body images from vehicle control (left panel) and BG45 (50 mg/kg; right panel) groups after 3-week treatment.

Table 1

IC50 values of BG45 against the deacetylase activity of recombinant HDAC1–3 and HDAC6.

HDAC1	HDAC2	HDAC3	HDAC6
2.0 μM	2.2 μM	289 nM	>20 μM

Table 2

MS275 and BG45 with bortezomib triggers synergistic cytotoxicity in RPMI8226 cells.

A

Merck60 (μM)	Bortezomib (nM)	CI
1	2	1.95
1	3	1.06
1	4	1.19
2	2	1.54
2	3	1.21
2	4	1.34
3	2	1.45
3	3	1.4
3	4	1.55

B

MS275 (μM)	Bortezomib (nM)	CI
1	2	0.57
1	3	0.66
1	4	0.81
2	2	0.56
2	3	0.63
2	4	0.76
3	2	0.53
3	3	0.62
3	4	0.77

C

BG45 (μM)	Bortezomib (nM)	CI
5	2	1.04
5	3	0.83
5	4	0.84
10	2	1.19
10	3	0.78
10	4	0.77
20	2	0.91
20	3	0.67
20	4	0.63

RPMI8226 cells were treated with Merck60 or MS275 or BG45 and/or bortezomib.

Cytotoxicity was assessed by MTT assay (mean ± SD; n=3).

Combination index (CI) was calculated using CompuSyn software. CK1 indicates synergistic effects.